Activation of the Flavoprotein Domain of gp91*phox* upon Interaction with N-Terminal p67*phox* (1−210) and the Rac Complex

Yukio Nisimoto,*,‡ Hisamitsu Ogawa,§ Kei Miyano,|| and Minoru Tamura||

Department of Biochemistry, Aichi Medical University, School of Medicine, Nagakute, Aichi 480-1195, Japan, Department of Biology, Fujita Health University School of Medicine, Toyoake, Aichi 470-1192, Japan, and Department of Applied Chemistry, Faculty of Engineering, Ehime University, Matsuyama, Ehime 790-8577, Japan

Received April 6, 2004; Revised Manuscript Received June 1, 2004

ABSTRACT: A series of truncated forms of His_6-tagged gp91*phox* were expressed, solubilized, and purified in the presence of 30 μM FAD. The truncated gp91*phox* with the longest sequence in the C-terminal region (221−570) (gp91C) showed the highest activity (turnover rate, 0.92) for NADPH diaphorase in the presence of either 0.3% Triton X-100 or 0.5% Genapol X-80. Activity was not inhibited by superoxide dismutase but was blocked by an inhibitor of the respiratory burst oxidase, diphenylene iodonium. The flavinated gp91C contained approximately 0.9 mol of FAD/mol of protein (MW 46 kDa) and 12% α-helix content. In the absence of p47*phox*, p67*phox* showed considerable activation of gp91C in the presence of Rac. Carboxyl-terminal truncated p67*phox* (1−210) (p67N), which is the minimal active fragment, was fused with Rac or Q61LRac. The fusion protein p67N-Rac (or p67N-Q61LRac) showed a 2-fold higher stimulatory effect on NBT reductase activity of gp91C than the combination of the individual cytosolic p67N and Rac proteins. In contrast, Rac-p67N, a fusion with the opposite orientation, showed a smaller significant effect on the enzyme activity. The EC_{50} values for p67*phox*, p67N, p67N-Rac, and Rac-p67N were 8.00. 4.35, 2.56, and 15.2 μM, respectively, while the K_m value for NADPH in the presence and absence of the cytosolic components was almost the same (40−55 μM). In the presence of Rac, p67N or p67*phox* bound to gp91C with a molar ratio of approximately 1:1 but neither p67N nor Rac alone showed significant binding.

Upon ingestion of microbes, neutrophils undergo a marked increase in oxygen consumption, a process referred to as the respiratory burst (*1*). The respiratory burst oxidase is a multicomponent enzyme that catalyzes the transfer of electrons from NADPH to O_2 to form superoxide (O_2^-). The essential membrane-associated core component is flavocytochrome b_{558} (*2*), which is composed of the glycoprotein gp91*phox* (*3*) and a 22 kDa protein, p22*phox* (*4*). Flavocytochrome b_{558} contains nonidentical hemes and FAD in a molar ratio of 2:1, and its large subunit, gp91*phox*, has candidate consensus binding sequences for pyridine nucleotide and flavin (*5*−*9*). Both hemes were recently shown to reside entirely in gp91*phox* (*10*). Thus, gp91*phox* is the catalytic center that transfers electrons from NADPH to O_2, and the other components can be considered to be regulatory. When the flavocytochrome is purified from neutrophil plasma membranes, the flavin dissociates and activity is lost, but activity and FAD binding can be restored by incubating the enzyme with phospholipids and FAD (*5*, *7*, *8*). Direct binding of native FAD and FAD analogues to flavocytochrome b_{558} has been demonstrated by several groups (*7*, *8*, *11*). Localization of the FAD binding region is predicted from studies using plasma membranes from chronic granulomatous disease with a point mutation at His-338, which showed low FAD content in the plasma membrane and failed to produce superoxide (*12*).

Various models (*10*, *13*) suggest that the heme groups both reside within the hydrophobic N-terminal half of the molecule, and specific histidine residues within this region have been suggested to be heme ligands. The relatively hydrophilic C-terminal half of gp91*phox* is homologous to several flavoprotein dehydrogenases, particularly in putative FAD and NADPH binding sequences (*5*−*7*) (Figure 1), and is therefore predicted to form an independently holding flavoprotein domain. The location of the NADPH binding site is not well established. Although gp91*phox* contains regions homologous to known NADPH binding sites (Figure 1), direct binding of NADPH or $NADP^+$ has not been demonstrated. Different affinity labeling analogues of NADPH show binding to either gp91*phox* (*14*, *15*) or p67*phox* (*16*−*18*). The latter result has led to the suggestion that p67*phox* contains the binding site for pyridine nucleotide and that activation might involve bringing this binding site into juxtaposition with the flavin moiety on the flavocytochrome (*16*−*18*). In a previous study (*19*), the genetically engineered flavoprotein-homologous domain of gp91*phox* (residues 306−570), which eliminated the hydrophobic transmembrane heme-containing domain, showed very weak NADPH diaphorase activity, indicating that the flavoprotein-homologous domain contains both the NADPH and FAD binding sites.

* To whom correspondence should be addressed. Tel: 0561-62-3311. Fax: 0561-61-4056. E-mail: nisiio@aichi-med-u.ac.jp.
‡ Aichi Medical University.
§ Fujita Health University School of Medicine.
|| Ehime University.

10.1021/bi0400249 CCC: $27.50 © 2004 American Chemical Society
Published on Web 07/02/2004

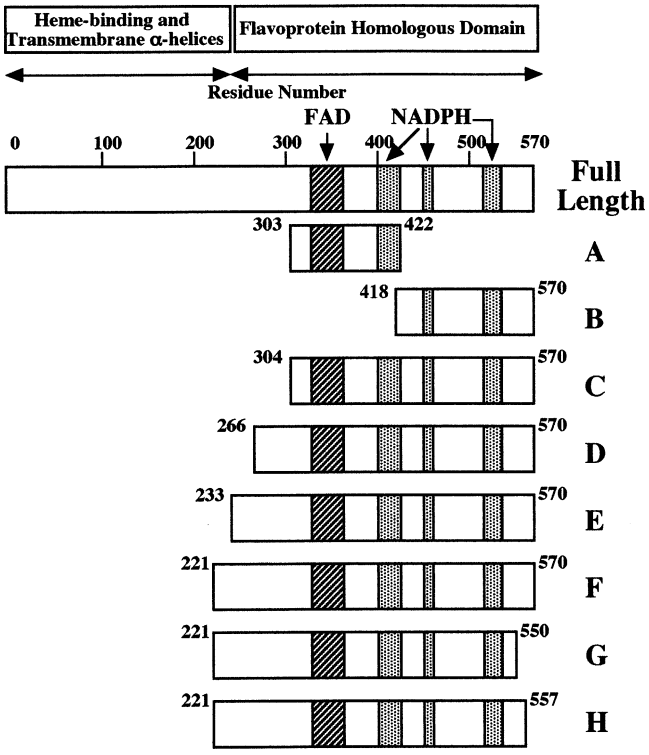

FIGURE 1: Truncated gp91*phox* containing the flavoprotein-homologous domain expressed in *E. coli*. The putative FAD binding region (hatched bars) and regions implicated in NADPH binding (gray bars) are indicated. A series of truncated forms indicated by eight bars (A−H) were constructed as N-terminal His_6-tagged proteins.

The flavocytochrome shows little or no oxidase activity in the absence of the cytosolic regulatory proteins p47*phox*, p67*phox*, and Rac, a small GTP binding protein (*20*−*24*). Upon cell activation by exposure to bacteria or chemical activators, these proteins assemble on the plasma membrane in a 1:1:1 ratio with flavocytochrome b_{558}, and superoxide generation was greatly induced (*25*−*27*). In addition, a cell-free NADPH diaphorase activity of flavocytochrome b_{558} as well as NADPH oxidase activity was markedly stimulated upon interaction with p67*phox* protein (*28*). With regard to the role of cytosolic oxidase proteins in the activation, the following points have been noted: (i) Rac and p67*phox* are the minimum activating components (*29*, *30*) that regulate FAD reduction *(13*), and (ii) p47*phox* functions as an adapter protein to interact with p67*phox* as well as p22*phox*, and it regulates the heme reduction (*13*). In recent results pointing to p67*phox*, Han et al. (*31*) identified an activation domain within p67*phox* that is essential for NADPH oxidase activity. Truncation mutants identified this region within residues 199−210, and a single point mutation at residue 204 completely eliminated NADPH oxidase activity without affecting specific interactions of p67*phox* with p47*phox* or Rac (*31*). In addition, we provided evidence that the activation domain on p67*phox* regulates the reduction of FAD by NADPH but does not affect the binding of NADPH itself, which is consistent with the regulation of hydride/electron transfer rate from NADPH to FAD (*32*). The fusion protein of p67N[1] (1−210) with Rac has also greatly stimulated the cell-free NADPH oxidase activity (*33*, *34*).

To directly prove the interactions between the flavoprotein domain of gp91*phox* and cytosolic proteins, we prepared a series of truncated forms of gp91*phox* and p67N fusion proteins. On the basis of kinetic and binding assays, we examined the effects of p67*phox* and p67N nonfusion and fusion proteins on the NADPH diaphorase activity in the flavoprotein domain of gp91*phox*. Our present results indicate that the C-terminal region (residues 221−570) of gp91*phox* offers the domain for both FAD and NADPH binding sites and responds to catalytic regulation by p67*phox* and Rac in the absence of p47*phox*.

MATERIALS AND METHODS

Materials. pGEX-2T, pGEX-6P, PreScission protease, *Escherichia coli* BL21 strain, and glutathione−Sepharose were purchased from Amersham Pharmacia Biotech (Little Chalfond, U.K.). Oligonucleotide primers used were synthesized by the same manufacturer. *Eco*RI, *Bam*HI, and *Hin*dIII were purchased from Toyobo Inc. (Tokyo, Japan). pET-30a(+), pET-30b(+), and pET-30c(+) vectors were obtained from Novagen. The PCR purification kit, Ni-NTA agarose, and His_6 antibody were from Qiagen GmbH. Rac antibody was purchased from Cytoskelton, Inc. (Denver, CO). Genapol X-80 and Triton X-100 were from Calbiochem, and sodium *N*-dodecanoylsarcosinate and DFP were from Wako Chemical Co. (Tokyo, Japan). Cytochrome *c*, NBT, FAD, NADPH, GTPγS, imidazole, and protease inhibitor cocktail were obtained from Sigma Aldrich (St. Louis, MO).

Truncation Mutations of gp91phox. A series of truncated gp91*phox* clones were obtained by PCR using gp91*phox* cDNA cloned in the pGEX-2T plasmid (Pharmacia Biotech) as the template. According to previous methods (*19*), PCR products for eight lengths of truncate gp91*phox* (303−422, 418−570, 304−570, 265−570, 233−570, 221−570, 221−550, and 221−557) were purified with a PCR purification kit (Qiagen). The purified DNA fragments were ligated into the *Bam*HI and *Hin*dIII sites of the pET-30(+) vector (Novagen) and then transformed into BL21(DE3). Transformants were selected from LB/kanamycin plates, and plasmids were isolated from 2 mL cultures of transformants as described previously (*19*). The plasmids were digested with *Bam*HI and *Hin*dIII and were separated on 1% agarose to confirm the presence of the insert. The clones were sequenced to rule out unexpected mutation and to confirm the truncations.

Expression and Purification of Truncated gp91phox. For preparation of His_6-truncated gp91*phox*, *E. coli* were grown at 37 °C in LB media (1 L) to an A_{550nm} of 0.6. Isopropyl β-D-thiogalactoside (1 mM) was added, and the cells were shaken at 37 °C for 4 h. All of the truncated forms of gp91*phox* were initially insoluble. These were solubilized and renatured according to a modification of the method of Misawa et al. (*35*). Cells were pelleted by centrifugation at 4500g for 15 min, resuspended in buffer A [50 mM Hepes, pH 7.4, containing 0.15 M NaCl, 1 mM $MgCl_2$, 30 μM FAD,

[1] Abbreviations: NBT, nitroblue tetrazolium; PCR, polymerase chain reaction; IPTG, isopropyl β-D-thiogalactopyranoside; DFP, diisopropyl fluorophosphate; PIPES, piperazine-*N*,*N*′-bis(2-ethanesulfonic acid); SOD, superoxide dismutase; DPI, diphenylene iodonium; *phox*, phagocyte oxidase; gp91C, N-terminal-truncated gp91*phox* (residues 221−570); p67N, C-terminal-truncated p67*phox* (residues 1−210); CGD, chronic granulomatous disease.

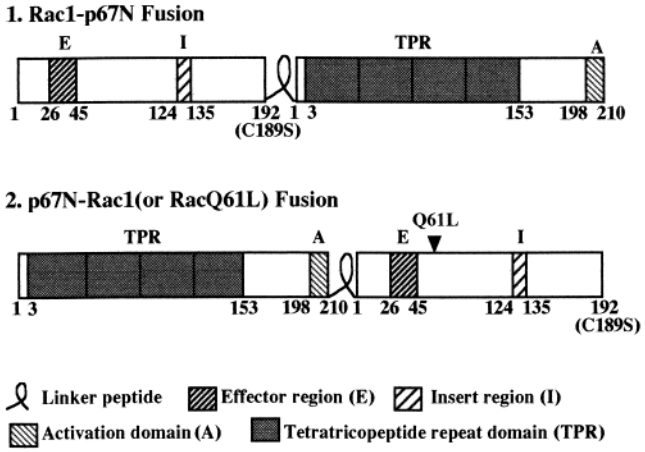

FIGURE 2: Schematic drawing of fusion proteins between N-terminal p67*phox* and Rac1. C-Terminal truncated p67*phox* (1−210) fusion proteins were prepared in this study. A tetratricopeptide repeat (TPR) and an activation domain (A) were shown in p67N. An effector region (E) and an insert region (I) are indicated in Rac. A fusion protein consisting of p67N and constitutively active Rac (Q61L mutant indicated by an arrow) as well as wild-type Rac was expressed. Each p67N fusion has a linker peptide, Ser-Glu-Phe.

2 μg/mL protease inhibitor cocktail, 1 μM DFP, and 8 M urea (or 0.5% sodium *N*-dodecanoylsalcosinate) containing 20 mM imidazole], and sonicated at 3 °C for 15 s (three times). Insoluble material was removed by centrifugation at 50000g for 1 h. The supernatant was applied to nickel chelate affinity beads, which were washed three times with several volumes of wash buffer (buffer A containing 40 mM imidazole). The column was further washed with 50 mM sodium phosphate buffer, pH 7.4, containing 0.15 M NaCl, 1 mM $MgCl_2$, 2 μg/mL protease inhibitor cocktail, 1 μM DFP, 30 μM FAD, and 0.5% Genapol X-80 (buffer B). The protein was eluted with buffer B containing 250 mM imidazole, and fractions with NBT reductase activity were pooled. The truncated gp91*phox* proteins were subjected to the assay for NADPH diaphorase activity and to SDS−PAGE.

Preparation of Rac, p67N (1−210), p67phox, and p47phox. Complementary DNAs encoding human Rac [Rac1(C189S)] and p67N were gifts from Dr. David J. Lambeth (Department of Pathology, Emory University School of Medicine). The protein Rac1 (C189S) is referred to as wild-type Rac in this paper. We constructed the RacQ61L mutant on the basis of Rac1 (C189S), which is fully active and more stable than natural Rac1. The pGEX-2T plasmid containing the cDNA for Rac, p67N, or p67*phox* was transfected into BL21 cells. The proteins were expressed and purified with glutathione−Sepharose beads. Human full-length p47*phox* protein was a generous gift from Dr. David Lambeth (Department of Pathology, Emory University School of Medicine).

Expression of Fusion Proteins. As shown in Figure 2, construction of recombinant plasmids for three fusion proteins, p67N-Rac, p67N-RacQ61L, and Rac-p67N, was performed by previously described methods (*33*). The linker peptide encoded between p67N and Rac was Ser-Gln-Phe. The fusion proteins were expressed in *E. coli* at 37 °C for 2.5 h after addition of IPTG. The cells were frozen in the absence of glycerol and thawed immediately before use to improve the recovery. The purification was carried out by glutathione−Sepharose column chromatography. Fusion proteins with single major bands at an expressed molecular mass (approximately 45 kDa) on SDS−PAGE were stored at −75 °C.

NADPH-Dependent Diaphorase Activity Assay. NBT and cytochrome *c* reductase activities were measured according to the previously described method (*19*). The activities for eight kinds of truncated gp91*phox* were assayed in a 1 mL volume of assay buffer (0.3% Triton X-100, 50 mM NaCl, 4 mM $MgCl_2$, 20 μM FAD in 50 mM phosphate buffer, pH 7.3) containing 0.1 mM NBT (or 0.1 mM cytochrome *c*). The final concentration of 0.5% Genapol X-80 was also used in the assay instead of 0.3% Triton X-100. The reaction was initiated by the addition of 0.2 mM NADPH at 37 °C. To examine the effects of cytosolic regulatory proteins, gp91C was preincubated with a combination of cytosolic components (p67*phox* plus Rac, p67N plus Rac, p67N-Rac, p67N-RacQ61L, or Rac-p67N) at 4 °C for 15 min. Rac was preloaded with 10 μM GTPγS just before the assay. At the end of the preincubation period, an aliquot of the preincubation mixture was taken out and added to the above assay buffer with or without superoxide dismutase (80 units). The rate of NBT reduction was quantified by monitoring the absorbance change at 595 nm using an extinction coefficient of 12.6 $mM^{-1}\cdot cm^{-1}$ at 595 nm (*36*). After the addition of NADPH, the duration of the NBT reductase assay was 10 min since the absorbance change at 595 nm was almost linear throughout this interval. An extinction coefficient of 18.5 $mM^{-1}\cdot cm^{-1}$ at 550 nm was used to calculate the quantity of cytochrome *c* reduced (*37*).

Spectrophotometric Assay. The FAD content of gp91C flavinated in the renaturation process was estimated by absorption and fluorescence spectra. Spectrophotometric assay of FAD was carried out using an extinction coefficient of 11.3 $mM^{-1}\cdot cm^{-1}$ at 450 nm (*38*). The fluorescence spectrum was measured using a Hitachi Model F-3000 spectrofluorometer, with an excitation wavelength of 450 nm and an emission wavelength of 525 nm. Circular dichroism spectra of gp91C were monitored at 16 °C in a Jasco J-720 WI spectrophotometer equipped with a data processor for CD, Jasco Model j-DPZ. For the far-UV region, a cell with a path length of 1 mm was used, and the protein concentration was in the range of 0.5−1.0 mg/mL.

Western Blot Analysis. Proteins separated by SDS−PAGE (10% or 14% gel) were transferred to an Immobilon-P membrane (Millipore Corp., Bedford, MA). The membrane was incubated at 25 °C for 2 h in 4% skim milk in 20 mM phosphate buffer, pH 7.3, containing 0.14 M NaCl and 2.7 mM KCl. Antibodies used were those to the His_6 tag, p67*phox*, and Rac1. After washing, the membrane was reacted with antibodies (3.0 μg/mL) and then with horseradish peroxidase-linked secondary antibody (IgG, 1:5000 dilution). The Immobilon-P membrane was washed extensively three times with 20 mM phosphate-buffered saline, pH 7.3, containing 0.1% Tween 20 (20 min each). The Western blots were stained for 5 min with 3,3′-diaminobenzidine in 20 mM phosphate-buffered saline, pH 7.3, containing 0.03% H_2O_2.

RESULTS

Expression of His_6-Tagged Forms of Truncated gp91phox. The expression strategy was designed on the basis of the

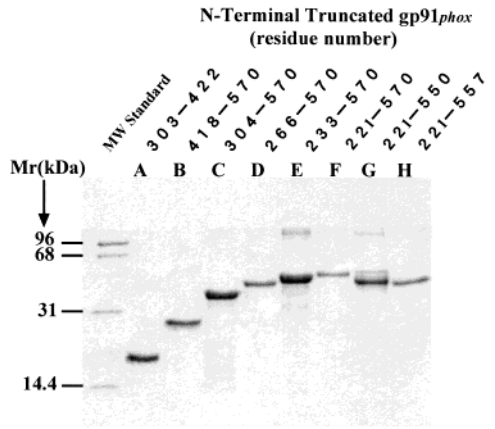

FIGURE 3: SDS−PAGE of expressed His_6-fusion forms of truncated gp91*phox*. The His_6-fusion forms of truncated gp91*phox* were expressed in *E. coli*, purified, and renatured in the presence of 30 μM FAD on a Ni^{2+}-chelating column as described in Materials and Methods. The purified proteins (approximately 5 μg) were loaded onto 10% (w/v) SDS−PAGE gel.

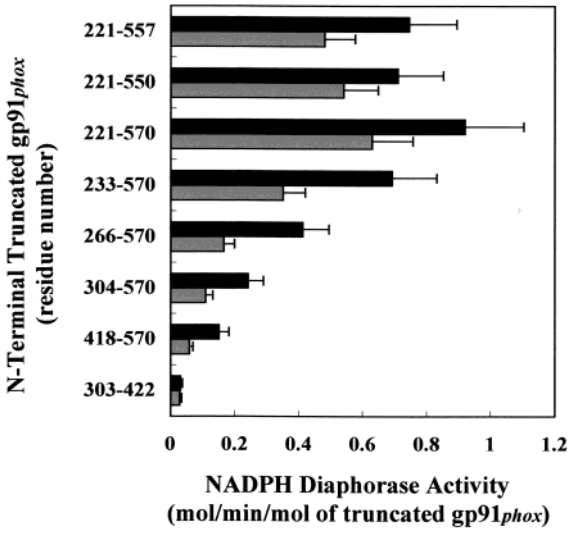

FIGURE 4: NADPH-dependent diaphorase activity of truncated gp91*phox*. Each form of deleted gp91*phox* (50 μg) was assayed for NBT (black bars) and cytochrome *c* (gray bars) reductase activities. The reaction was initiated by the addition of 0.2 mM NADPH to 1 mL of reaction mixture described in Materials and Methods. The average and standard error of a minimum of three determinations are shown.

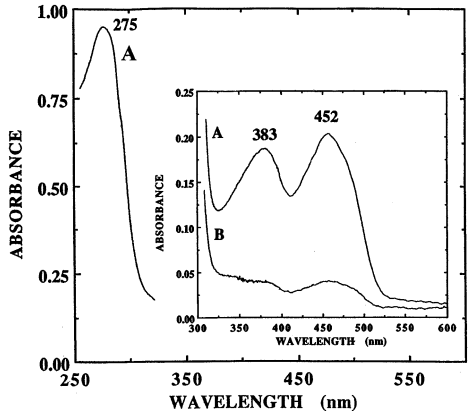

FIGURE 5: Absorption spectrum of flavinated gp91C. The gp91C protein, which was purified in the presence of 8 M urea, 30 μM FAD, protease inhibitor cocktail, and 10 μM DFP, was immediately renatured according to the methods described in Materials and Methods. Inset: Enlarged absorption spectra of flavinated gp91C protein (0.93 mg/mL) in the visible region. Curve A: gp91C refolded and flavinated in the Ni-NTA column. Curve B: gp91C refolded and flavinated by the dialysis method.

idea that the C-terminal half of the gp91*phox* protein is relatively hydrophilic and that this domain will fold independently. We initially constructed a series of truncated mutants as N-terminal His_6-fusion proteins. Those were truncated gp91*phox* (303−422), (418−570), (304−570), (266−570), (233−570), (221−570), (221−550), and (221−557). All constructs were expressed at high levels in *E. coli*, and they were solubilized using a urea (or sodium *N*-dodecanoylsarcosinate) unfolding/refolding method. The proteins were purified under denaturing conditions on a Ni^{2+} chelate affinity matrix. All purified proteins corresponded in size to their predicted molecular masses on SDS−PAGE. In the absence of detergent, the purified truncate gp91*phox* proteins quickly showed turbid forms that appeared to be aggregates of four or more monomers. However, when the truncated gp91*phox* (221−570) protein was treated with 0.3% Triton X-100 or 0.5% Genapol X-80, 70% or more of it migrated as a monomeric molecular size of about 58 kDa on Sephacryl S-300 column chromatography equilibrated with the buffer containing the above detergent (data not shown). The eight kinds of truncated proteins that appeared to be eluted at their monomeric states on the size column showed molecular masses of 19.0, 23.2, 36.0, 40.9, 44.3, 45.7, 43.6, and 44.3 kDa, respectively, on a 10% SDS−PAGE gel (Figure 3). Figure 4 shows the NADPH-dependent diaphorase activity of each truncated gp91*phox* using NBT or cytochrome *c* as an electron acceptor. In accord with the previous report (*19*), NBT reduction gave the highest turnover rate among several electron acceptors investigated. The longest form of fusion, His_6-gp91C, showed the highest NADPH-dependent NBT and cytochrome *c* reductase activities. These activities were not affected by deletion of C-terminal segments (558−570 and 551−570) of gp91C (Figure 4). As compared with the diaphorase activity of general flavoenzymes, the maximal rates of NBT and cytochrome *c* reduction of gp91C were significantly slower, about 0.92 electron min^{-1} (molecule of gp91C)$^{-1}$, compared with 6.5 for the intact flavocytochrome b_{558}, and they were not inhibited by SOD. The gp91C protein with highest NADPH diaphorase activity among the eight forms of truncated gp91*phox* was used to clarify its catalytic properties and interaction with cytosolic regulatory proteins.

Spectral Properties of Flavinated gp91C. Truncated gp91C was solubilized and purified in the presence of 30 μM FAD and 8 M urea and was finally refolded in the Ni-NTA column by changing the wash buffer containing 8 M urea to one containing 0.5% Genapol X-80. After removal of free FAD by Sephadex G-25, a stable absorption spectrum was obtained. The absorption spectrum of flavinated gp91C with three major peaks at 452, 383, and 275 nm can be seen in Figure 5 (spectrum A), and FAD was quantified by spectrophotometric and fluorometric assays. The flavin content was approximately 0.90 $\pm$ 0.05 mol/mol of protein. These results suggest that the truncated gp91*phox* has a relatively high affinity for FAD and that the flavinated protein shows catalytic activity. As shown in Figure 6, the flavinated gp91C

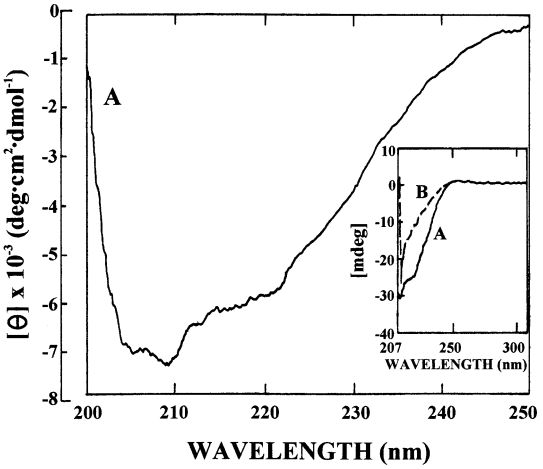

FIGURE 6: Far-ultraviolet CD spectra of gp91C. Renatured and flavinated gp91C protein (0.93 mg/mL) in the presence of 0.5% of Genapol X-80, protease inhibitor cocktail, and 10 μM DFP was measured (spectrum A). The following experimental parameters were used for the spectra: time constant, 1 s; repeat times, 10; scan speed, 100 nm/min; light path, 1 mm; scan range, 200−250 nm. Inset: The far-UV circular dichroism spectrum of gp91C was measured in the presence of 8 M urea (spectrum B), and spectrum A is a renatured form of gp91C.

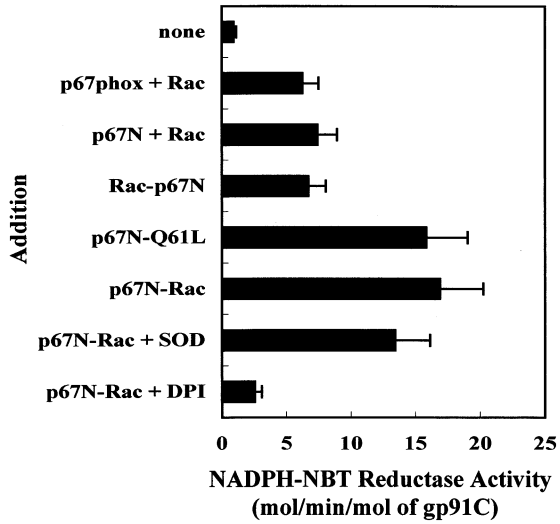

FIGURE 7: Effects of p67N fusion and nonfusion proteins on the NBT reductase activity of gp91C. The truncated gp91*phox* (4.5 μM) was preincubated with 15.2 μM p67*phox* or 13.5 μM p67N nonfusion and 20 μM Rac in 0.12 mL of medium (25 mM phosphate buffer, pH 7.3, containing 20 μM FAD and 10 μM GTPγS) at 4 °C for 15 min. Fusion protein (14.5 μM Rac-p67N, 14.8 μM p67N-Rac, or 15.0 μM p67N-RacQ61L) was preincubated with 4.5 μM gp91C without added Rac in 0.12 mL of the same medium as described above. Using 0.1 mL of the incubated mixture, NBT reduction was monitored at 595 nm at 37 °C. The reaction was started by adding 0.2 mM NADPH to 1 mL of the assay buffer in the presence or absence of either 80 units of SOD or 0.1 mM DPI. Error bars show the standard error of the mean ($n = 3$).

in the presence of 0.5% Genapol X-80 gave a CD spectrum with negative bands at 220 and 209 nm in the far-UV region (spectrum A). This form has about 12% of α-helical structure as estimated by the method of Greenfield and Fasman (*39*). The truncated gp91C treated gradually with an increasing concentration of urea (4−8 M) showed significant decreases in the ellipticity of both the 220 and 209 nm bands, and no remarkable negative peak due to the helical conformation of the peptide chain was observed in the presence of 8 M urea (spectrum B in Figure 6 inset).

The flavin content of this FAD-reconstituted gp91C was greatly decreased up to 0.19 ± 0.05 mol of FAD/mol of protein when dialysis was carried out for its renaturation after being released from the Ni-NTA bead column (spectrum B in Figure 5 inset). The flavinated gp91C with its approximate molecular mass of 46 kDa is susceptible to proteolysis even in the presence of protease inhibitors, resulting in the appearance of 26 and 20 kDa bands that time-dependently increased during the dialysis for 16 h at 3 °C. Upon prolonged incubation of gp91C at 3 °C for 1 week, the 46 kDa protein was completely cleaved to the two fragments (data not shown). In parallel with the increased amount of the two bands, NADPH diaphorase activity of gp91C was reduced. Since the flavinated gp91C easily underwent autolysis during storage, it was used for experiments immediately after the preparation.

NADPH-Dependent Diaphorase Activities of His$_6$-gp91C. The flavinated gp91C, which has a stoichiometry of FAD binding to protein at nearly a 1:1 mol ratio, shows NBT reduction without added FAD in the assay medium. However, the reduction rate was gradually decreased in the prolonged catalytic reaction over 10 min at 37 °C, probably because of dissociation of flavin from the protein. The gp91C exhibits hyperbolic kinetics with respect to NADPH in the NBT reductase assay, and its maximal activity increased nearly 5-fold in the presence of detergent added to the assay system. The K_m value for NADPH in the presence of 0.3% Triton X-100 or 0.5% Genapol X-80 was determined to be 55 ± 10.5 μM from Lineweaver−Burk plots. This value is similar to the K_m for NADPH (approximately 50 μM) observed in the intact phagocyte NADPH oxidase (*15*); however, a considerably larger value for NADPH (0.12 mM) was obtained in the absence of the detergent. As mentioned above, since the truncated gp91*phox* is highly aggregative and is assumed to reaggregate in the detergent-free medium, Triton X-100 (or Genapol X-80) was added to the assay medium to increase the monomeric state of gp91C, resulting in a rise in affinity for NADPH in a flavin-occupied catalytic center. Thus, the entire assay for NADPH diaphorase activity of gp91C protein was performed in the presence of the detergent.

At high concentrations, Rac together with either p67*phox* or p67N in the absence of p47*phox* supports full activation in a cell-free NADPH oxidase reconstitution system (*31*, *40*). In addition, p67N-Rac fusion protein also showed marked stimulation of NADPH oxidase activity reconstituted in a cell-free system lacking p47*phox* (*33*, *34*). To investigate the intermolecular interactions between the C-terminal flavoprotein domain of gp91*phox* and cytosolic factors, NADPH-dependent NBT reductase activity of gp91C was assayed after its preincubation with the cytosolic fusion or nonfusion proteins (Figure 7). The NADPH-dependent NBT reductase activity of gp91C increased 16-fold or more upon incubation with p67N-Rac or p67N-RacQ61L preloaded with GTPγS. Compared with the fused forms, in the presence of Rac, p67*phox* and nonfused p67N showed 6.5- and 7.5-fold increases of the NBT reductase activity, respectively. Activity was dependent upon gp91C, and the cytosolic proteins alone showed little or no activity. The activation by Rac-p67N fusion protein was only 38% of that with p67N-Rac fusion. Thus, the N-terminal region of p67*phox* and/or Rac interact

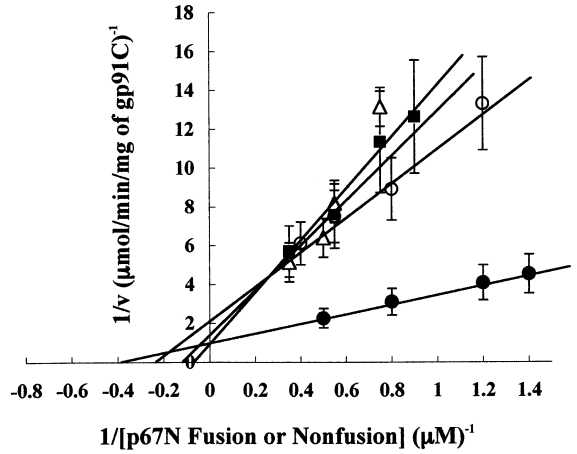

FIGURE 8: Concentration dependence of p67N fusion and nonfusion proteins in the stimulation of NBT reductase activity of gp91C. Data are plotted in Lineweaver−Burk format. The concentration of either p67N (0.85−2.50 μM, open circles) or p67*phox* (1.10−2.85 μM, closed squares) was varied as indicated in the presence of 3.50 μM Rac. The concentrations of p67N-Rac fusion (closed circles) and Rac-p67N fusion (open triangles) were changed from 0.70 to 2.00 μM and from 1.35 to 2.85 μM, respectively. Truncated gp91C (15 μg, 0.33 nmol) was preincubated with p67*phox* and p67N nonfusion or fusion proteins in 1 mL of the assay buffer at 4 °C for 15 min. The NBT reduction was started by adding 0.2 mM NADPH to the incubation mixture. Error bars show the standard error of the mean ($n = 3$).

Table 1: Kinetic Parameters of Fused, Nonfused p67N, and p67*phox* in NADPH-Dependent NBT Reductase Activity of gp91C[a]

addition	EC_{50} (μM)	V_{max} [μmol min^{-1} (mg of gp91C)$^{-1}$]	K_m(NADPH) (μM)
p67*phox* + Rac	8.00 ± 0.70	0.66 ± 0.05	46 ± 5.8
p67N + Rac	4.35 ± 0.50	0.44 ± 0.04	43 ± 5.5
p67N-Rac (fused)	2.56 ± 0.25	1.05 ± 0.12	40 ± 5.2
Rac-p67N (fused)	15.2 ± 2.0	1.03 ± 0.10	52 ± 5.8
none		0.02 ± 0.005	55 ± 10.5

[a] EC_{50} and V_{max} values were obtained graphically as in Figure 8. K_m was determined by a double reciprocal plot of initial velocity versus NADPH concentrations at each fixed concentration of either p67N fusion, nonfusion, or p67*phox* in the presence of Rac preloaded with 10 μM GTPγS.

with the C-terminal region of gp91*phox* and participate in the activation of NADPH diaphorase. It has recently been reported that the activation domain (residues 199−210) of p67*phox* regulates electron transfer from NADPH to flavin, and Val-204 plays a crucial role in the step (*31*). However, p67*phox* (V204A), which contains a point mutation in the activation domain and is completely inactive in the cell-free NADPH oxidase assay (*31*), was ineffective in stimulating diaphorase activity (data not shown). This result suggests that the p67*phox*-Rac complex is activating the flavoprotein domain of gp91C by a mechanism different from that for the holoprotein.

To further examine the effects of fusion on the concentration dependence for the cytosolic components, the NBT reductase activity was measured with various concentrations of fused or nonfused components (Figure 8 and Table 1). The EC_{50} values for p67*phox*, nonfused p67N, p67N-Rac, and Rac-p67N fusions were determined from Lineweaver−Burk plots to be 8.00, 4.35, 2.56, and 15.2 μM, respectively. Fusion proteins showed a little higher V_{max} value than those for p67*phox* and p67N nonfusion proteins. These results

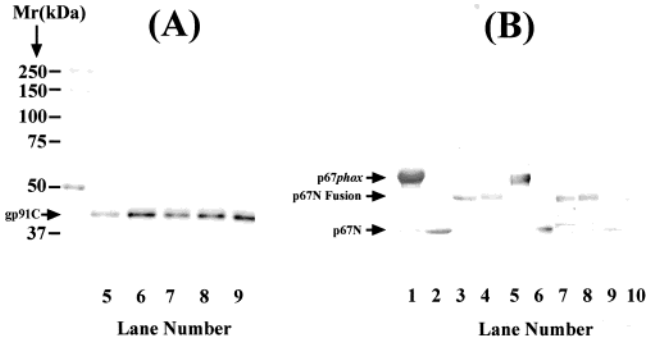

FIGURE 9: Interaction between gp91C and cytosolic proteins. Purified gp91C (3.0 nmol) was incubated with p67N-Rac (15 nmol), Rac-p67N (15 nmol), p67N (15 nmol) plus Rac1 (20 nmol), or p67*phox* (15 nmol) plus Rac1 (20 nmol) in the presence of 10 μM GTPγS at 25 °C for 10 min. After preincubation, each mixture was adjusted to 1 mL by 50 mM phosphate buffer, pH 7.3, containing 0.1 mM NBT, 20 μM FAD, 0.3% Triton X-100, 50 mM NaCl, 4 mM $MgCl_2$, and 10 μM GTPγS (reaction buffer). After the diaphorase reaction was started by addition of 0.2 mM NADPH, the reaction mixture was applied to a Ni^{2+}-NTA column (5 × 8 mm), and Ni^{2+} beads were washed well with a 20-fold excess of the above reaction buffer. Proteins were eluted by 1 mL of the reaction buffer containing 250 mM imidazole. Eluted proteins were separated by SDS−PAGE and subjected to immunoblot by using antibodies to His_6 (panel A) and to p67*phox* (panel B), respectively. The positions of gp91C (panel A) and cytosolic components (panel B) were indicated by arrows. Lanes 1, 2, 3, and 4 show authentic p67*phox*, p67N, p67N-Rac, and Rac-p67N proteins (10 μg each), respectively. Lane 5 shows p67*phox* plus Rac; lane 6, p67N plus Rac; lane 7, p67N-Rac fusion; lane 8, Rac-p67N fusion; lane 9, p67N alone. The cytosolic proteins (15 nmol each) without added gp91C were mixed and loaded to a Ni^{2+}-NTA column as a control test (lane 10). The lane numbers (5−9) on panel A correspond to those on panel B. The numbers on the left side of panel A exhibit molecular mass standards.

suggest that a fusion p67N-Rac improves the affinity for gp91C as compared with nonfusion p67N and p67*phox*, while Rac-p67N lowers the affinity. The K_m values for NADPH were determined with the NBT reductase activated by p67N-Rac fusion and the nonfused components. The K_m values with the fused and nonfused proteins ranged from 40 to 52 μM (Table 1). This indicated that fusion between p67N and Rac does not have much effect on the NADPH binding site located in gp91C. The EC_{50} and V_{max} values were not markedly affected by the superoxide dismutase added to the assay medium (Figure 7), indicating that NBT reduction is not brought about by the superoxide anion. Thus, it seems likely that NBT accepts electrons directly from the reduced FAD. Diphenylene iodonium, a known inhibitor of NADPH-dependent superoxide generation by the intact phagocyte oxidase (*41*), blocked NADPH-dependent NBT reduction greater than 80% as shown in Figure 7. These catalytic properties suggest that the flavoprotein domain of gp91C achieves a more or less native structure following the expression, purification, and renaturation processes.

Binding of p67N or p67phox to gp91C. Interactions between C-terminal gp91*phox* and p67N fusion or nonfusion protein were detected in the NBT reductase reaction of gp91C. Just after the catalytic reaction was started by addition of NADPH, the reaction mixture was loaded onto a Ni^{2+}-NTA bead column and washed, and then the immobilized proteins were eluted with 250 mM imidazole. The pooled eluates were subjected to Western blot analysis (Figure 9). As shown in Figure 9B, p67N fusion, nonfusion, and

p67*phox* proteins bind to gp91C in the presence of Rac (GTPγS); however, the intermolecular binding was less significant in the absence of Rac (lane 9). Little or no nonspecific binding of the cytosolic components to Ni^{2+} beads was observed (lane 10). Together with the kinetic and Western blot data, this indicates that gp91C in the presence of Rac binds to p67N fusion or nonfusion proteins. Binding brings about the activation of the flavin binding catalytic site of gp91*phox*. Although it is stated that Rac interacts with the assembled oxidase through the insert region (*42*, *43*), its direct binding to gp91C is not observed in the present assay (data not shown).

DISCUSSION

We supported the idea that gp91*phox* is the only redox component and is composed of a flavoprotein-homologous domain containing NADPH and FAD binding sites plus a hydrophobic domain possessing two heme binding sites. The former domain shows NADPH dehydrogenase activity that is regulated by p67*phox* (*31*, *32*). On the basis of previous models, the C-terminal globular portion of the gp91*phox* subunit is largely exposed to the cytosolic solvent and is accessible to NADPH from the cytoplasm (*44*). Several flavin-dependent reductases possess a β-stranded barrel structure for FAD binding (*45*, *46*). The sequence alignment of the FAD binding domain of gp91*phox* and the ferredoxin−$NADP^+$ reductase family has shown that amino acid sequence 279−400 of gp91*phox* is homologous to a general FAD binding structure (*12*). Recently, it was reported that the H338Y mutation of gp91*phox* found in a rare X-linked form of CGD led to complete depletion of FAD and no detectable superoxide-generating activity (*12*). The HPFT motif (residues 338−341) in this structure is predicted to interact directly with FAD in the flavocytochrome model (*4*) and is conserved in the human, porcine, and mouse gp91*phox* (*47*, *48*). In fact, in a previous study (*19*) we expressed a thioredoxin-truncated gp91*phox* (306−570) fusion protein. Its catalytic activity was extremely low and dependent upon FAD, which showed a lower binding affinity (K_d 0.74 mM) compared with 50 μM for the native flavocytochrome b_{558} (*49*). In addition, the diaphorase activity of the truncated gp91*phox* (306−570) was little affected by the interactions with p67*phox* containing the activation domain and Rac, which were essential for NADPH oxidase activation in a reconstituted cell-free system (*31*). From these data it was assumed that the catalytically inefficient activation by the p67*phox*-Rac complex may be due to the absence of an appropriate conformation of the flavoprotein domain to bind with the cytosolic components. To solve this problem, the present study successfully prepared a flavinated C-terminal gp91*phox* protein, gp91C, with a longer sequence (residues 221−570) that possesses most of the predicted β-stranded barrel structure, including the HPFT motif, and also contains regions that are predicted to form the FAD and NADPH binding sites.

In contrast to gp91*phox* (306−570), the gp91C that solubilized and purified in the presence of FAD showed an absorption spectrum of flavinated protein (FAD/protein = approximately 1:1 binding ratio) and NBT reductase activity, which was observed without added FAD in the assay system. In the presence of Rac, the diaphorase was markedly stimulated by p67*phox* or p67N, which contains the activation and Rac binding domains, but the effects of p47*phox* and truncated p47*phox* (residues 1−268) were less significant. The previous study (*32*) used kinetic deuterium isotope effects to demonstrate that the activation domain of p67*phox* regulates the reduction of FAD and does not affect NADPH binding affinity in a cell-free NADPH oxidase. In view of these results, the activation of NADPH diaphorase activity of gp91C induced by p67*phox* and Rac can also be ascribed to an increased rate of electron transfer between the two nucleotides, although its turnover rate was much lower than the superoxide-generating activity. As shown in Figure 10, we speculate that binding of the p67*phox*-Rac or p67N-Rac complex functions as a molecular switch to cause a conformational change in the flavoprotein domain of gp91*phox*, which allows hydride ion transfer from NADPH to FAD. The kinetic scheme shows the fact that the p67*phox*-Rac complex activates both diaphorase activity and NADPH oxidase activity by requiring a regulated step common to both kinetic cycles, yet the turnover for diaphorase activity is much slower than oxidase activity. It seems that this can be explained by a partially rate-limiting (slow) dissociation of $NADP^+$ from the E-$FADH_2$ enzyme that limits turnover rate in the diaphorase reaction but a non-rate-limiting dissociation of $NADP^+$ from E-FAD in the oxidase reaction.

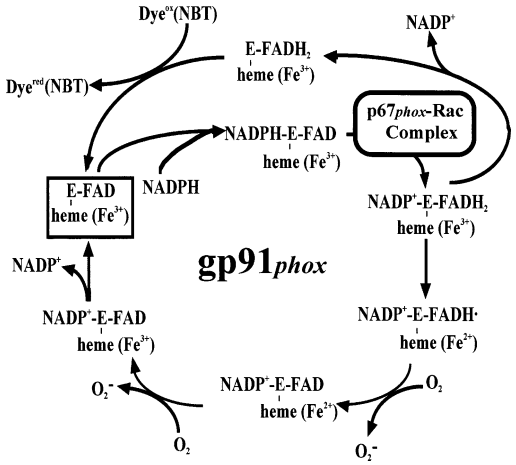

FIGURE 10: Hypothetical scheme of intramolecular electron flow linked to NADPH dehydrogenase and oxidase reactions of gp91*phox* regulated by the p67*phox*-Rac complex.

In addition, we observed nearly equimolar binding of gp91C upon direct interaction with the p67N and Rac complex. Since p67*phox* and p67N failed to stimulate NBT reductase activity in the absence of Rac, Rac may work synergistically with p67*phox* in activating the diaphorase activity of the flavoprotein domain by binding to the N-terminal TPR region of p67*phox*, producing an active conformation. In these protein−protein interactions, the p67N-Rac fusion form caused an increased affinity for gp91C as compared with the nonfused individual components. Rac is known to bind to the plasma membrane through its C-terminal region (*50*) and to bind to p67*phox* via its N-terminal effector region (residues 26−45) (*51*−*53*, *42*). A third region on Rac, the insert region (residues 124−135), is essential for optimal activity in vitro and appears to be involved in protein−protein interactions within the assembled oxidase (*42*, *43*). However, Rac alone can hardly bind to the flavoprotein domain of gp91*phox* (data not shown). Thus, the p67N-Rac binary complex may orient in such a way as

to position its activation domain (residues 199−210) in proximity to nucleotide binding sites, thereby activating the electron flow between NADPH and FAD. Previous studies (*33*, *34*) suggested that p67N, which was stably bound to gp91*phox* through activated Rac or RacQ61L, prevented FAD dissociation from an active site of flavinated flavocytochrome b_{558} and stabilized the oxidase complex. These results also confirm the concept that p67N and Rac are minimal essential effectors for the activation of the flavoprotein domain and that p47*phox* functions as an adapter protein to produce the fully activated oxidase complex.

ACKNOWLEDGMENT

We thank Dr. Toshiya Endo of Nagoya University Graduate School of Science for many technical suggestions on the CD experiments. We are also indebted to Dr. David J. Lambeth of Emory University School of Medicine for helpful discussions and reagents.

REFERENCES

1. Segal, A. W. (1987) Absence of both cytochrome b_{-245} subunits from neutrophils in X-linked chronic granulomatous disease, *Nature 326*, 88−91.
2. Segal, A. W., and Jones, O. T. G. (1987) Novel cytochrome *b* system in phagocytic vacuoles of human granulocytes, *Nature 276*, 515−517.
3. Dinauer, M. C., Orkin, S. H., Brown, R., Jesaitis, A. J., and Parkos, C. A. (1987) The glycoprotein encoded by the X-linked chronic granulomatous disease locus is a component of the neutrophil cytochrome *b* complex, *Nature 327*, 717−720.
4. Parkos, C. A., Dinauer, M. C., Walker, L. E., Rodger, A. A., Jesaitis, A. J., and Orkin, S. H. (1988) Primary structure and unique expression of the 22-kilodalton light chain of human neutrophil cytochrome *b*, *Proc. Natl. Acad. Sci. U.S.A. 85*, 3319−3323.
5. Segal, A. W., West, I., Wientjes, F., Nugent, J. H. A., Chavan, A. J., Haley, B., Garcia, R. C., Rosen, H., and Scrace, G. (1992) Cytochrome b_{-245} in a flavocytochrome containing FAD and the NADPH-binding site of the microbicidal oxidase of phagocytes, *Biochem. J. 284*, 781−788.
6. Sumimoto, H., Sakamoto, N., Nozaki, M., Sakai, Y., Takeshige, K., and Minakami, S. (1992) Cytochrome b_{558}, a component of the phagocyte NADPH oxidase, is a flavoprotein, *Biochem. Biophys. Res. Commun. 186*, 1368−1375.
7. Rotrosen, D., Yeung, C. L., Leto, T. L., Malech, H. L., and Kwong, C. H. (1992) Cytochrome b_{558}: the flavin-binding component of the phagocyte NADPH oxidase, *Science 256*, 1459−1462.
8. Nisimoto, Y., Otsuka-Murakami, H., and Lambeth, D. J. (1995) Reconstitution of flavin-depleted neutrophil flavocytochrome b_{558} with 8-mercapto-FAD and characterization of the flavin-reconstituted enzyme, *J. Biol. Chem. 270*, 16428−16434.
9. Cross, A. R., Rae, J., and Curnutte, J. T. (1995) Cytochrome b_{-245} of the neutrophil superoxide-generating system contains two nonidentical hemes. Potentiometric studies of a mutant form of gp91*phox*, *J. Biol. Chem. 270*, 17075−17077.
10. Yu, L., Quinn, M. T., Cross, A. R., and Dinauer, M. C. (1998) Gp91phox is the heme binding subunit of the superoxide-generating NADPH oxidase, *Proc. Natl. Acad. Sci. U.S.A. 95*, 7993−7998.
11. Doussiere, J., Buzunet, G., and Vignais, P. V. (1995) Photoaffinity labeling and photoinactivation of the O_2^--generating oxidase of neutrophils by an azido derivative of FAD, *Biochemistry 34*, 1760−1770.
12. Yoshida, L. S., Saruta, F., Hikawa, Y., Tatsuzawa, O., and Tsunawaki, S. (1998) Mutation at histidine 338 of gp91phox deletes FAD and affects expression of cytochrome b_{558} of the human NADPH oxidase, *J. Biol. Chem. 273*, 27879−27886.
13. Cross, A. R., and Curnutte, J. T. (1995) The cytosolic activating factors p47phox and p67phox have distinct roles in the regulation of electron flow in NADPH oxidase, *J. Biol. Chem. 270*, 6543−6548.
14. Ravel, P., and Lederer, F. (1993) Affinity-labeling of an NADPH-binding site on the heavy subunit of flavocytochrome b_{558} in particulate NADPH oxidase from acdtivated human neutrophils, *Biochem. Biophys. Res. Commun. 196*, 543−552.
15. Doussiere, J., Brandolin, G., Derrien, V., and Vignais, P. V. (1993) Critical assessment of the presence of an NADPH binding site on neutrophil cytochrome b_{558} by photoaffinity and immunochemical labeling, *Biochemistry 32*, 8880−8887.
16. Smith, R. M., Connor, J. A., Chen, L. M., and Babior, B. M. (1996) The cytosolic subunit p67phox contains an NADPH-binding site that participates in catalysis by the leukocyte NADPH oxidase, *J. Clin. Invest. 98*, 977−983.
17. Dang, P. M. C., Babior, B. M., and Smith, R. M. (1999) NADPH dehydrogenase activity of p67*phox*, a cytosolic subunit of the leukocyte NADPH oxidase, *Biochemistry 38*, 5746−5753.
18. Dang, P. M. C., Johnson, J. L., and Babior, B. M. (2000) Binding of nicotinamide adenine dinucleotide phosphate to the tetratricopeptide repeat domains at the N-terminus of p67*phox*, a subunit of the leukocyte nicotinamide adenine dinucleotide phosphate oxidase, *Biochemistry 39*, 3069−3075.
19. Han, C.-H., Nisimoto, Y., Lee, S. H., Kim, E. T., Lambeth, J. D. (2001) Characterization of the Flavoprotein Domain of gp91*phox* Which Has NADPH Diaphorase Activity, *J. Biochem. 129*, 513−520.
20. Volpp, B. D., Nauseef, W. M., and Clark, R. A. (1988) Two cytosolic neutrophil oxidase components absent in autosomal chronic granulomatous disease, *Science 242*, 1295−1297.
21. Leto, T. L., Lomax, K. J., Volpp, B. D., Nunoi, H., Sechler, J. M. G., Nauseef, W. M., Clark, R. A., Gallin, J. I., and Malech, H. L. (1990) Cloning of a 67-kD neutrophil oxidase factor with similarity to a noncatalytic region of p60c-src, *Science 248*, 727−730.
22. Lomax, K. J., Leto, T. L., Nunoi, H., Gallin, J. I., and Malech, H. L. (1989) Recombinant 47-kilodalton cytosol factor restores NADPH oxidase in chronic granulomatous disease, *Science 245*, 409−412.
23. Abo, A., Pick, E., Hall, A., Totty, N., Teahan, C. G., and Segal, A. W. (1991) Activation of the NADPH oxidase involves the small GTP-binding protein p21 rac1, *Nature 353*, 668−670.
24. Knaus, U. G., Heyworth, P. G., Evans, T., Curnutte, J. T., and Bokoch, G. M. (1991) Regulation of phagocyte oxygen radical production by the GTP-binding protein Rac2, *Science 254*, 1512−1515.
25. Uhlinger, D. J., Tyagi, S. R., Inge, K. L., and Lambeth, J. D. (1993) The respiratory burst oxidase of human neutrophils. Guanine nucleotides and arachidonate regulate the assembly of a multicomponent complex in a semirecombinant cell-free system, *J. Biol. Chem. 268*, 8624−8631.
26. Abrams, C. S., Zhao, W., Belmonte, E., and Brass, L. F. (1995) Protein kinase C regulates pleckstrin by phosphorylation of sites adjacent to the N-terminal pleckstrin homology domain, *J. Biol. Chem. 270*, 23317−23321.
27. Quinn, M. T., Evans, T., Loetterle, L. R., Jesaitis, A. J., and Bokoch, G. M. (1993) Translocation of Rac correlates with NADPH oxidase activation. Evidence for equimolar translocation of oxidase components, *J. Biol. Chem. 268*, 20983−20987.
28. Cross, A. R., Yarchover, J. L., and Curnutte, J. T. (1994) The superoxide-generating system of human neutrophils prossesses a novel diaphorase activity. Evidence for distinct regulation of electron flow within NADPH oxidase by p67*phox* and p47*phox*, *J. Biol. Chem. 269*, 21448−21454.
29. Freeman, J. L. R., and Lambeth, J. D. (1996) NADPH oxidase activity is independent of p67*phox in vitro*, *J. Biol. Chem. 271*, 22578−22582.
30. Koshkin, V., Lotan, O., and Pick, E. (1996) The cytosolic component p47*phox* is not a sine qua non participant in the activation of NADPH oxidase but is required for optimal superoxide producdtion, *J. Biol. Chem. 271*, 30326−30329.
31. Han, C.-H., Freeman, J. L. R., Lee, T., Motalebi, S. A., and Lambeth, J. D. (1998) Regulation of the neutrophil respiratory burst oxidase. Identification of an activation domain in p67*phox*, *J. Biol. Chem. 273*, 16663−16668.
32. Nisimoto, Y., Motalebi, S., Han, C.-H., and Lambeth, J. D. (1999) The p67*phox* activation domain regulates electron flow from NADPH to flavin in flavocytochrome b_{558}, *J. Biol. Chem. 274*, 22999−23005.
33. Miyano, K., Ogasawara, S., Han, C.-H., Fikuda, H., and Tamura, M. (2001) A fusion protein between Rac and p67*phox*(1−210)

reconstitutes NADPH oxidase with higher activity and stability than the individual components, *Biochemistry 40*, 14089−14097.
34. Miyano, K., Fukuda, H., Ebisu, K., and Tamura, M. (2003) Remakable stabilization of neutrophil NADPH oxidase using RacQ61L and a p67*phox*-p47*phox* fusion protein, *Biochemistry 42*, 184−190.
35. Misawa, S., and Kumagai, I. (1999) Refolding of therapeutic proteins produced in *Escherichia coli* as inclusion bodies, *Biopolymers 51*, 297−307.
36. Mitchell, J. A., Kolhaas, K. L., Matsumoto, T., Pollock, J. S., Forstermann, U., Warner, T. D., Schmidt, H. H., and Murad, F. (1992) Induction of NADPH-dependent diaphorase and nitric oxide synthase activity in smooth muscle and cultured macrophages, *Mol. Pharmacol. 41*, 1163−1168.
37. Tauber, A. J., and Goetzl, E. J. (1979) Structural and catalytic properties of the solubilized superoxide-generating acdtivity of polymorphonuclear leukocytes. Solubilization, stabilization in solution, and partial characterization, *Biochemistry 18*, 5576−5584.
38. Koziol, J. (1971) Fluorometric analysis of riboflavin and its coenzymes, *Methods Enzymol. 18B*, 253−285.
39. Greenfield, N., and Fasman, G. D. (1969) Computed circular dichroism spectra for the evaluation of protein conformation, *Biochemistry 8*, 4108−4116.
40. Kreck, M. L., Freeman, J. L. R., Abo, A., and Lambeth, J. D. (1996) Membrane association of Rac is required for high activity of the respiratory burst oxidase, *Biochemistry 35*, 15683−15692.
41. Nomanbhoy, T. K., and Cerione, R. A. (1996) Characterization of the interaction between RhoGDI and Cdc42Hs using fluorescence spectroscopy, *J. Biol. Chem. 271*, 10004−10009.
42. Nisimoto, Y., Freeman, J. L. R., Motalebi, S. A., Hirshberg, M., and Lambeth, J. D. (1997) Rac binding to p67*phox*. Structural basis for interactions of the Rac1 effector region andinsetregion with components of the respiratory burst oxidase, *J. Biol. Chem. 272*, 18834−18841.
43. Freeman, J. L. R., Abo, A., and Lambeth, J. D. (1996) Rac "insert region" is a novel effector region that is implicated in the activation of NADPH oxidase, but not PAK65, *J. Biol. Chem. 271*, 19794−19802.
44. Cross, A. R., and Jones, O. T. G. (1986) The effect of the inhibitor diphenylene iodonium on the superoxide-generating system of neutrophils. Specific labeling of a component polypeptide of the oxidase, *Biochem. J. 237*, 111−116.
45. Taylor, W. R., Jones, D. T., and Segal, A. W. (1993) A structural model for the nucleotide binding domains of the flavocytochrome b_{-245} beta-chain, *Protein Sci. 2*, 1675−1685.
46. Nishida, H., Inaka, K., and Miki, K. (1995) Specific arrangement of three amino acid residues for flavin-binding barrel structures in NADH-cytochrome b_5 reductase and the other flavin-dependent reductases, *FEBS Lett. 361*, 97−100.
47. Zhou, Y., Lin, G., and Murtaugh, M. P. (1995) Interleukin-4 supresses the expression of macrophage NADPH oxidase heavy subunit (gp91*phox*), *Biochim. Biophys. Acta 1265*, 40−48.
48. Bjorgvinsdottir, H., Ling, Z., and Dinauer, M. C. (1996) Cloning of murine gp91*phox* cDNA and functional expression in a human X-linked chronic granulomatous disease cell line, *Blood 87*, 2005−2010.
49. Koshkin, V., and Pick, E. (1994) Superoxide production by cytochrome b_{558}. Mechanism of cytosol-independent activation, *FEBS Lett. 328*, 285−289.
50. Kreck, M. L., Uhlinger, D. J., Tyagi, S. R., Inge, K. L., and Lambeth, J. D. (1994) Participation of the small molecular weight GTP-binding protein Rac1 in cell-free activation and assembly of the respiratory burst oxidase, *J. Biol. Chem. 269*, 4161−4168.
51. Diekmann, D., Abo, A., Johnson, C., Segal, A., and Hall, A. (1994) Interaction of Rac with p67*phox* and regulation of phagocytic NADPH oxidase activity, *Science 265*, 531−533.
52. Dorseuil, O., Reibel, L., Bokoch, G. M., Camonis, J., and Gacon, G. (1996) The Rac target NADPH oxidase p67*phox* interacts preferentially with Rac2 rather than Rac1, *J. Biol. Chem. 271*, 83−88.
53. Ahmed, S., Prigmore, E., Govind, S., Veryard, C., Kozma, R., Wientjes, F. B., Segal, A. W., and Lim, L. (1998) Cryptic Rac-binding and p21 (Cdc42Hs/Rac)-activated kinase phosphorylation sites of NADPH oxidase component p67*(phox)*, *J. Biol. Chem. 273*, 15693−15701.

BI0400249